energies

Article

Techno-Economic Evaluation of a Compressed CO_2 Energy Storage System for Load Shifting Based on Dynamic Modelling

Bin Zhang [1], Junbo Yang [1], Sule Tian [1], Qingxi Huang [2,*], Wei Wang [2,*], Qie Sun [2] and Xiaohan Ren [2]

[1] Shandong Electric Power Engineering Consulting Institute Co., Ltd., Jinan 250013, China; zhangbin@sdepci.com (B.Z.); yangjunbo@sdepci.com (J.Y.); tiansule@sdepci.com (S.T.)
[2] Institute of Thermal Science and Technology, Shandong University, Jinan 250061, China; qie@sdu.edu.cn (Q.S.); renxh@sdu.edu.cn (X.R.)
* Correspondence: qingxihuang.sdu@gmail.com (Q.H.); wangwei2023@sdu.edu.cn (W.W.)

Abstract: To reduce the electricity grid's valley—peak difference, thereby resulting in a smoother electricity load, this study employs a compressed CO_2 energy storage system to facilitate load shifting. Load shifting by the CCES system not only enhances the energy flexibility of the electricity load but also creates energy arbitrage from variations in the electricity prices. An optimization model is developed to optimize the operation of the CCES system to minimize the standard deviation of the electricity load. Thereby, load shifting by the CCES system can be achieved. Based on the real electricity loads and prices, results indicate that, with an energy storage capacity of 267 MWh, the CCES system can provide 3845 MWh, 4052 MWh, and 3816 MWh of upward flexible energy and 3846 MWh, 3180 MWh, and 3735 MWh of downward flexible energy during a week in summer, winter, and the transition season, respectively. With a lifespan of 35 years, the CCES system can attain a net present value (NPV) of MUSD 239.9 and a payback time of 2 years. The sensitivity analysis shows that increasing the energy storage capacity of the CCES system augments both the upward and downward flexible energy of the electricity load but reduces the NPV of the CCES system.

Keywords: compressed CO_2 energy storage system; load shifting; mixed integer non-liner programming; flexibility

check for updates

Citation: Zhang, B.; Yang, J.; Tian, S.; Huang, Q.; Wang, W.; Sun, Q.; Ren, X. Techno-Economic Evaluation of a Compressed CO_2 Energy Storage System for Load Shifting Based on Dynamic Modelling. *Energies* **2023**, *16*, 7894. https://doi.org/10.3390/en16237894

Academic Editor: Vanessa Fierro

Received: 18 October 2023
Revised: 21 November 2023
Accepted: 27 November 2023
Published: 3 December 2023

1. Introduction

The intermittency and the fluctuating nature of renewable energy result in grid instability when the penetration of renewable energy, typically wind and solar power, keeps increasing in the electricity system [1]. With the advancements in smart sensing and metering, energy generation technologies, and demand side management, energy storage technologies can help the grid to improve stability by optimizing supply and demand [2–4]. Recently, numerous forms of energy storage systems have been developed, including the following: pumped hydro energy storage (PHES) [5], compressed air energy storage (CAES) [6], compressed CO_2 energy storage (CCES) [7,8], and battery energy storage [9].

Among these energy storage systems, the PHES, the CAES, and the CCES systems can be installed on a large-scale installation [2]. The following benefits make the CCES an innovative and promising energy storage solution. First, the CCES system has excellent characteristics, such as environmental friendliness, high efficiency, economic viability, and no special geographical conditions [10]. Second, CO_2 is easier to condense to liquid since it has a higher dew point [11]. As a result, the pump can be utilized to compress CO_2 into greater pressure rather than a compressor, saving some electricity energy throughout the charging process [12]. Third, the CCES system can offer the potential for extensive CO_2 usage, which is conducive to reducing CO_2 emissions [11].

Recently, a growing number of studies have scrutinized the performance of the CCES system, underscoring its potential as a promising energy storage solution both in terms of steady state and in dynamic performance. In terms of the steady performance, Liu et al. [13]

conducted a thermodynamic and parametric analysis of the CCES system. They stated that the round trip efficiency (RTE) and the energy density of the CCES system in transcritical and supercritical states are, respectively, 63.4% and 497.7 kWh/m^3 and 62.3% and 255.2 kWh/m^3. Hao et al. [14] used the heat pump to recover the compression heat during the charging process to heat CO_2 during the discharging process. They proved that the round trip efficiency, the energy storage efficiency, and the heat storage efficiency increase with the increase in the energy storage pressure. Meanwhile, Xu et al. [15] compared the performance of the liquid CAES and CCES systems. They found that the liquid CAES system has higher round trip efficiency and energy efficiency, but the liquid CCES system has higher energy generated per unit volume. Wang et al. [16] optimized compressor outlet pressure, working fluid pump outlet pressure, turbine outlet pressure, evaporating pressure, turbine inlet temperature, and cold end temperature difference to maximize the RTE of the liquified CCES system using a genetic algorithm (GA). The result demonstrated that the RTE of the liquified CCES system can reach 56.6%.

In terms of the dynamic performance, Huang et al. [17] evaluated the dynamic operating characteristics of the CCES system in two operation modes, which were the basic operation mode and constant electric capacity mode. They found that the round trip efficiency of the CCES system varies from 16.7% to 56.7%. Zhang et al. [18] also evaluated the dynamic performance of the CCES system under sliding pressure operation. They found that the round trip efficiency of the CCES system under design conditions can reach 64.3%. Furthermore, Chaychizadeh et al. [19] conducted a dynamic simulation to evaluate the performance of the CCES system integrated with a wind farm. They stated that the system can properly work under 55.7–58.2% of the round trip efficiency.

Load shifting is a feasible method to achieve demand side management (DSM), which is beneficial in reducing the electricity grid's valley—peak difference, resulting in a smoother load and a solution for the investment of electricity transition and distribution lines under peak load [20]. By implementing the energy storage system in the demand side, load shifting can be achieved.

Numerous studies have recently focused on the load shifting by the energy storage systems, such as battery energy storage and thermal energy storage. Excellent load power fluctuation control is made possible by the battery's rapid charging and discharging capabilities. Han et al. [21] selected the type of battery and the optimized capacity of the batteries using the cooperative game model to maximize the performance of load shifting. David Parra et al. [22] also optimized the size of the battery to maximize the equivalent full cycles, the RTE, and the performance of load shifting.

The electricity load rises continuously in the summer due to the substantial increase in air conditioning usage for cooling, hence load shifting has been accomplished using thermal energy storage [23]. Ding et al. [24] used the particle swarm optimization algorithm to identify the thermal capacity and evaluated the performance of building thermal energy for load shifting. The result shows that, with an increase in the effective thermal capacity, the hourly load and the energy losses caused by load shifting strategies decrease. Load shifting can be achieved with battery and thermal energy storage, but their large-scale commercialization is constrained by their cost, life span, specific application scenarios, and application scale.

The literature review emphasizes the flexibility of load shifting by the energy storage system and highlights the necessity of optimizing the operation of the energy storage system for load shifting. The mechanical energy storage system includes the CCES system, which has the benefit of a long lifespan and greater installation capacity. Furthermore, the CCES system can be located in the transmission to provide service according to the grid needs [25]. In our previous study [26], we introduced a parameter, notably the state of charge (SOC), for optimizing the operation of the CCES system to create energy arbitrage. The results demonstrated that it is viable for the CCES system to participate in the electricity market. Consequently, the CCES system is perfectly suited to load shifting and can potentially achieve a better techno-economic outlook. However, the CCES system belongs to the mechanical energy storage system, which is different from the battery energy and the thermal energy storage systems, making the findings on other energy storage system operation optimizations inapplicable to the CCES system.

Therefore, this paper aimed to evaluate the techno-economic flexibility of the CCES system for load shifting. An optimization model was developed to optimize the operation strategy of the CCES system based on its dynamic characteristics. By implementing the operation strategy, this study explored the potential energy flexibility that the CCES system could offer for electricity load management as well as evaluated its net present value (NPV) and payback period. Additionally, sensitivity analysis was conducted to assess how the CCES system's energy storage capacity influences both the energy flexibility of the electricity load and the system's revenue.

The main contributions of this paper include: (1) a new application of the compressed CO_2 energy storage system; and (2) the techno-economic assessment of load shifting by the compressed CO_2 energy storage system based on dynamic modeling. The findings will contribute to a deeper comprehension of the compressed CO_2 energy storage system's practical applicability.

2. Problem Formulation

2.1. Optimization Objective

The grid operator aims for a more stabilized electricity load to mitigate frequent startups and shutdowns of conventional generators as well as to minimize spinning reserve capacity. Consequently, when the CCES system is employed to achieve load shifting, the objective function of the operation strategy optimization is to minimize the standard deviation of the electricity load [27], which is formulated as follows:

$$minimize\ \sigma_D = \sqrt{\frac{\sum\left(D^t + v_c^t \cdot W_{Comp}^t - v_d^t \cdot W_{Expa}^t - \frac{\sum D^t + v_c^t \cdot W_{Comp}^t - v_d^t \cdot W_{Expa}^t}{N}\right)}{N}} \quad (1)$$

where σ_D is the standard deviation of the electricity load; D^t is the initial electricity load; v_c^t and v_d^t are the unit state indicators for charging and discharging modes, respectively; W_{Comp}^t and W_{Expa}^t are the electric capacities of the compressor and the expander, respectively; N is the sample number; and superscript t denotes the scheduling time.

2.2. Constraints

The optimization problem necessitates the inclusion of the following constraints:

(1) Operation mode

The constraints regarding the operation mode are expressed as Formulas (2)–(4), which specifies that the CCES system only performs one operation mode from charging mode, discharging mode, and idle mode at a time.

$$v_c^t + v_d^t \leq 1 \quad (2)$$

$$v_c^t \in \{0, 1\} \quad (3)$$

$$v_d^t \in \{0, 1\} \quad (4)$$

(2) The SOC of the CCES system

The constraints regarding the SOC are expressed as Formulas (5) and (6), which denotes that the SOC at time t is between its minimum and its maximum value, and the SOC at time $t+1$ depends on the SOC at time t and the operation status of the CCES system, respectively.

$$SOC_{min} \leq SOC^t \leq SOC_{max} \quad (5)$$

$$SOC^{t+1} = SOC^{t} + v_c^t \frac{\dot{m}_{W_{Comp}}^t \cdot t_{st}}{M_{total}} - v_d^t \frac{\dot{m}_{W_{Expa}}^t \cdot t_{st}}{M_{total}} \quad (6)$$

where SOC_{min} is the minimum SOC of the CCES system; SOC_{max} is the maximum SOC of the CCES system; $\dot{m}_{W_{Comp}}^t$ is the mass flow rate of the compressor at time t; $\dot{m}_{W_{Expa}}^t$ is the mass flow rate of the expander at time t; and t_{st} is the duration of compression or expansion at the mass flow rate.

Based on our previous definition [26], the SOC for the CCES system is calculated as the ratio of the amount of stored working gas to the total amount of stored working gas, as shown in Formula (7).

$$SOC(t) = \frac{M(t)}{M_{total}} \quad (7)$$

where $M(t)$ is stored mass of CO_2 at time t; and M_{total} is total stored mass of CO_2 of the CCES system.

(3) Electric capacity of the compressor

The constraints regarding the electric capacity of the compressor are expressed as Formula (8) and Formula (9).

$$W_{Comp,min} \leq W_{Comp}^t \leq W_{Comp,max} \quad (8)$$

$$\frac{v_c^t \cdot \dot{m}_{W_{Comp}}^t \cdot t_{st}}{M_{total}} \leq SOC_{max}^{W_{Comp}} - SOC^t \quad (9)$$

where $W_{Comp,min}$ and $W_{Comp,max}$ are the minimum and the maximum values of the electric capacity of the compressor W_{Comp}^t; and $SOC_{max}^{W_{Comp}}$ is the maximum SOC of the CCES system at a given compressor's electric capacity W_{Comp}, which is determined as Formula (10).

$$SOC_{max}^{W_{Comp}} = \frac{\dot{m}_{W_{Comp}}^t \cdot t_{c,W_{Comp}}}{M_{total}} \quad (10)$$

where $t_{c,W_{Comp}}$ is the duration of the charging process when the CCES charges at W_{Comp}.

(4) Electric capacity of the expander

The constraints regarding the electric capacity of the expander are expressed as Formulas (11) and (12).

$$W_{Expa,min} \leq W_{Expa}^t \leq W_{Expa,max} \quad (11)$$

$$\frac{v_d^t \cdot \dot{m}_{W_{Expa}}^t \cdot t_{st}}{M_{total}} \leq SOC^t - SOC_{min}^{W_{Expa}} \quad (12)$$

where $W_{Expa,min}$ and $W_{Expa,max}$ are the minimum and the maximum values of the electric capacity of the expander W_{Expa}^t; and $SOC_{min}^{W_{Expa}}$ is the minimum SOC of the CCES system at a given expander's electric capacity W_{Expa}, which is determined as Formula (13).

$$SOC_{min}^{W_{Expa}} = \frac{M_{total} - \dot{m}_{W_{Expa}} \cdot t_{d,W_{Expa}}}{M_{total}} \quad (13)$$

where $t_{d,W_{Expa}}$ is the duration of the discharging process when the CCES system discharges at W_{Expa}.

2.3. Solving Method

The optimization problem is a mixed inter linear programming (MILP) problem, which is solved using Gurobi in this study.

3. Case Study

The definition of a case study is provided in this section in order to evaluate the techno-economic performance of the CCES system for load shifting.

3.1. The Electricity Price and Load Data

Three weeks randomly selected from summer, winter, and the transition season, respectively, are utilized to assess the techno-economic performance of the CCES system for load shifting. Figures 1–3 present the electricity price and load data for these weeks from the California electricity market [28], with standard deviations of the electricity load at 76.3, 66.2, and 71.6.

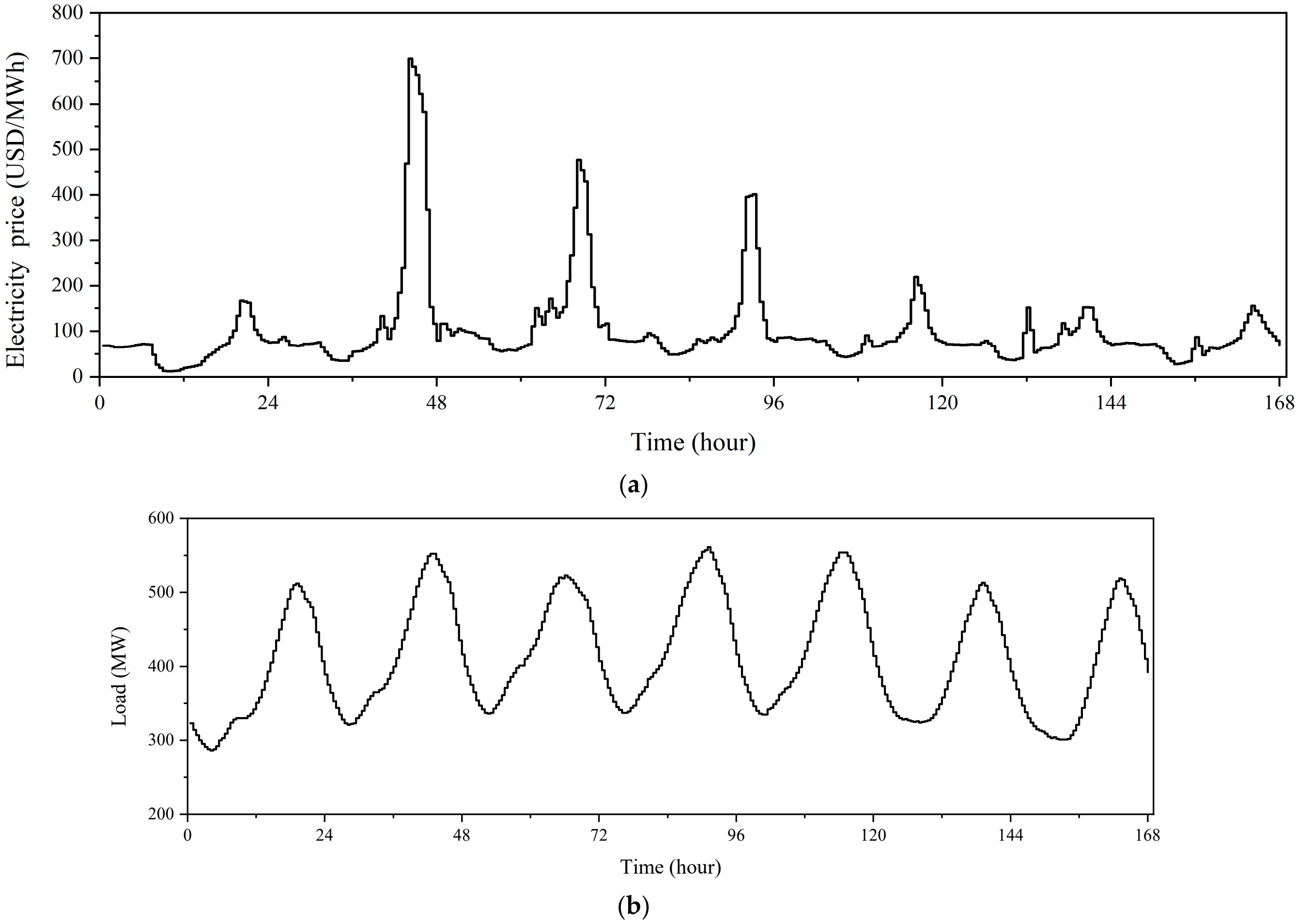

Figure 1. The electricity price and load during a week in summer [28]. (**a**) The electricity price during a week in summer. (**b**) The electricity load during a week in summer.

3.2. The Compressed Carbon Dioxide Energy Storage System

The schematic of the CCES system used in the study is shown in Figure 4, which consists of the low-pressure gas tank (LPT), the high-pressure gas tank (HPT), the compressor (Comp), the expander (Expa), the throttling valve (TV), the intercooler (IC), and the heater (HT).

Table 1 presents an overview of the CCES system's key parameters. The charging capacity ranges from 57 MW to 110 MW, while the discharging capacity spans from 30 MW to 120 MW. The CCES system's energy storage capacity is 267 MWh.

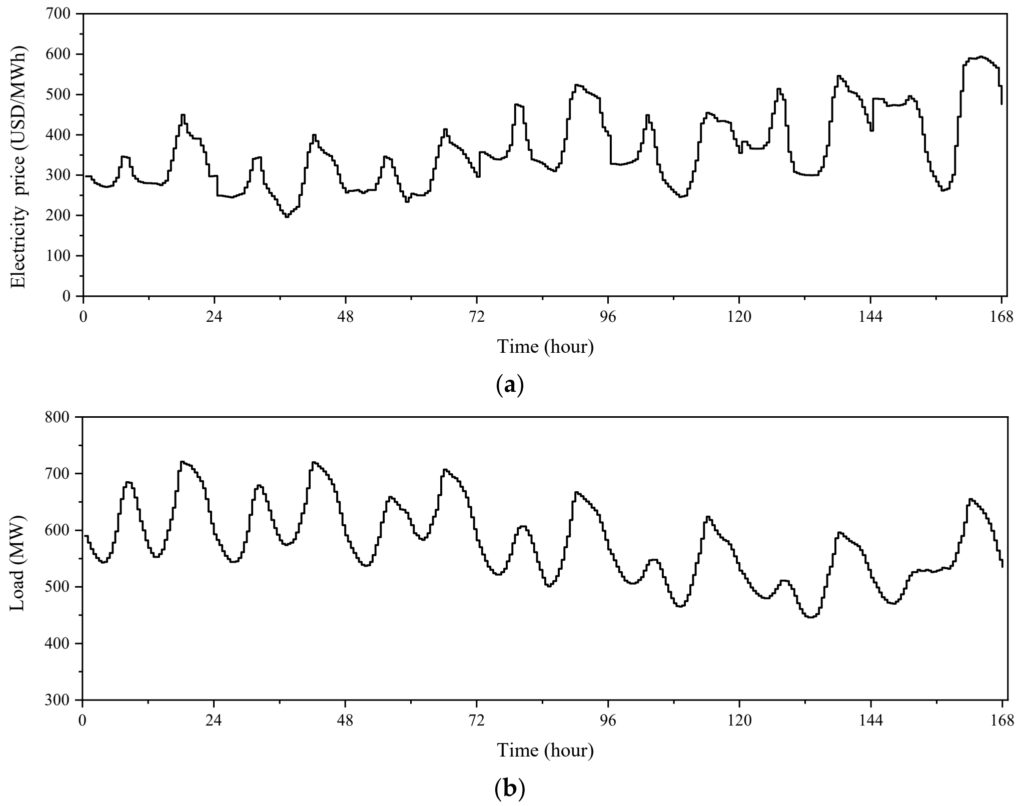

Figure 2. The electricity price and load during a week in winter [28]. (**a**) The electricity price during a week in winter. (**b**) The electricity load during a week in winter.

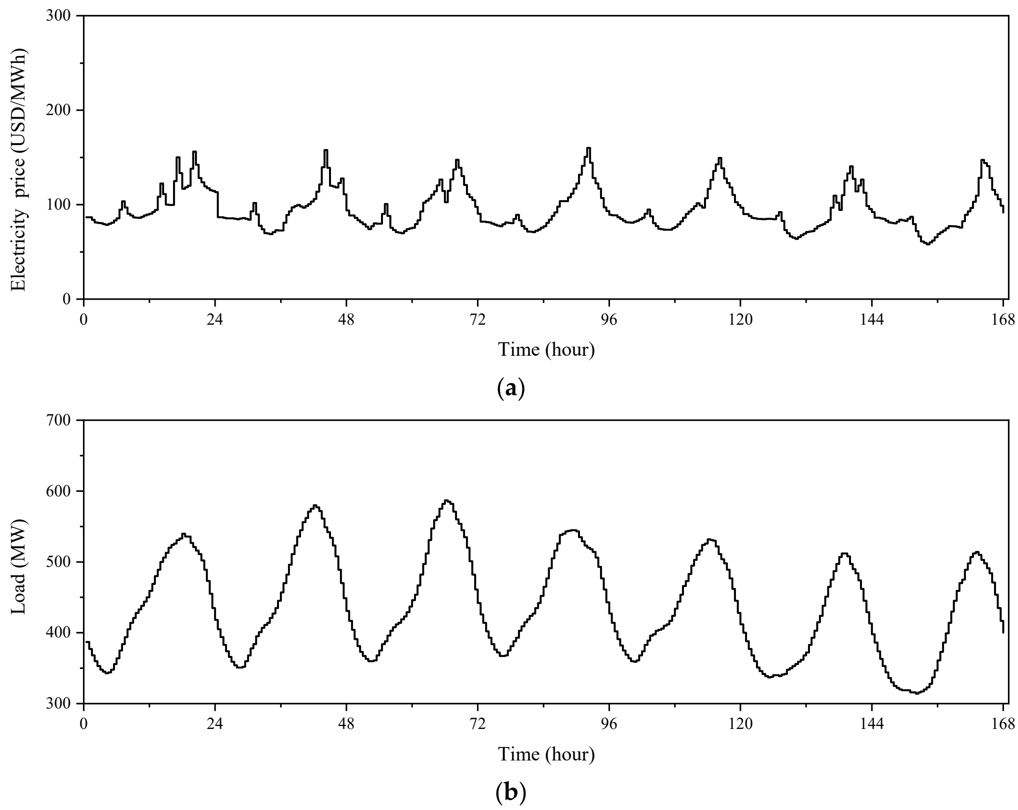

Figure 3. The electricity price and load during a week in transition season [28]. (**a**) The electricity price during a week in transition season. (**b**) The electricity load during a week in transition season.

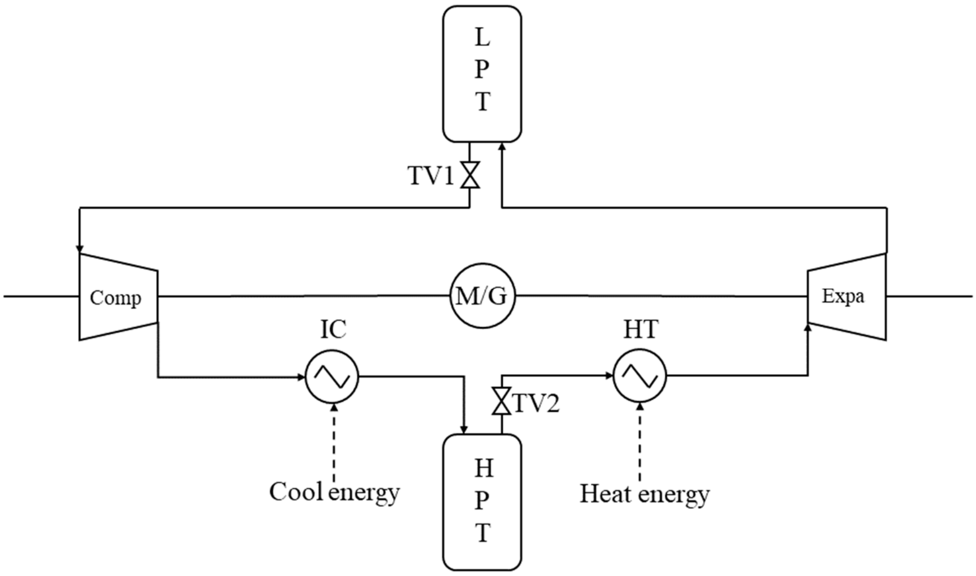

Figure 4. The schematic of the compressed CO_2 energy storage system [17].

Table 1. The main parameters of the CCES system [17].

Parameters	Value
Rated isentropic efficiency of compressor (%)	89
Rated isentropic efficiency of expander (%)	88
The volume of high-pressure gas tank (m^3)	7600
The volume of low-pressure gas tank (m^3)	36,000.00
The initial pressure of low-pressure gas tank (MPa)	1.0
The initial pressure of high-pressure gas tank (MPa)	2.3
Maximum pressure ratio of the compressor	7.8–14.0
Pressure ratio of the expander	4.5–10.1
Life cycle (years)	35
Investment cost (MUSD)	36.6

The CCES dynamic model was developed and validated in our previous study [17]. Based on the validated dynamic CCES model, Figures 5 and 6 illustrate the maximum SOC of the CCES system at different compressors' electric capacities and the minimum SOC of the CCES system at different expander's electric capacities, respectively.

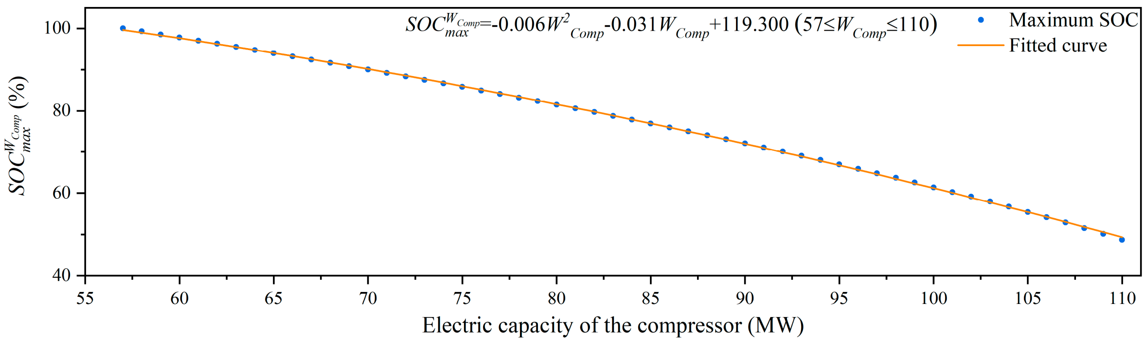

Figure 5. The maximum SOC of the CCES system at different compressor's electric capacities.

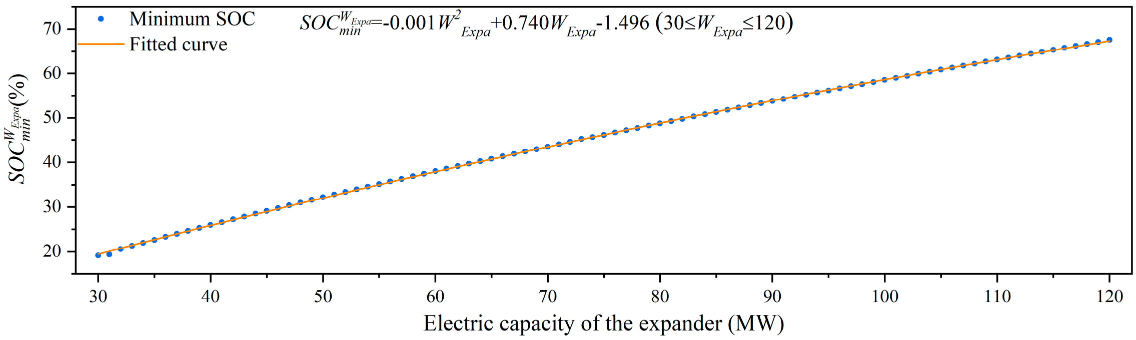

Figure 6. The minimum SOC of the CCES system at different expanders' electric capacities.

3.3. Key Performance Indicator

The key performance indicators (KPIs) used to evaluate the performance of the CCES system for load shifting include two parts: energy flexibility indicators and economic indicators.

3.3.1. Energy Flexibility Indicators

The energy flexibility is categorized into two types of scenarios: upward flexibility and downward flexibility.

The upward flexibility is the capability of the user to consume more energy when the grid confronts more power supply than its demand [29]. The maximum upward flexible capacity and the upward flexible energy are used to describe the upward flexibility, as shown in Formulas (14) and (15).

$$W_{fmax,up} = max(D_{ld}^t - D_{ref}^t) \tag{14}$$

$$E_{f,up} = \int_0^{t_{up}} (D_{ld}^t - D_{ref}^t)dt \tag{15}$$

where $W_{fmax,up}$ is the maximum upward flexible capacity; D_{ld}^t is the electricity load after load shifting; D_{ref}^t is the initial electricity load; E_f is the upward flexible energy; t_{up} is the duration of the CCES system providing upward flexibility; and superscript t denotes the scheduling time.

The downward flexibility is the capability of the user to consume less energy when the grid experiences lower power supply than its demand [29]. The maximum downward flexible capacity and the downward flexible energy are used to describe the downward flexibility, as shown in Formulas (16) and (17).

$$W_{fmax,down} = max(D_{ref}^t - D_{ld}^t) \tag{16}$$

$$E_{f,down} = \int_0^{t_{dowm}} (D_{ref}^t - D_{ld}^t)dt \tag{17}$$

where $W_{fmax,down}$ is the maximum downward flexible capacity; $E_{f,down}$ is the downward flexible energy; and t_{down} is the duration of the CCES system providing downward flexibility.

3.3.2. Economic Indicators

Net present value (NPV) and payback time are used as KPIs to evaluate the economy of the CCES system for load shifting. The NPV can be used to present the net profit of the system over life span, which is calculated as follows:

$$NPV = \sum \frac{CI_t - CO_t}{(1+d)^t} \tag{18}$$

where CI denotes cash inflows, which are from the income of selling electricity and coal reduction for load shifting, as shown in Formula (19); CO is cash outflows, which are from the outcome of buying electricity, as shown in Formula (20); t is the life span of the CCES system; and d denotes discount rate.

$$CI = \sum E_{Expa}^{t} \cdot p^{t} + K \cdot E_{Expa}^{t} \tag{19}$$

$$CO = \sum E_{Comp}^{t} \cdot p^{t} \tag{20}$$

where E_{Expa}^{t} and E_{Comp}^{t} are the energy capacities of the compressor and the expander, respectively; p^t is the electricity piece; and K is the specific coal consumption, as shown in Formula (21) [30].

$$K = k_0 + k_1 W_{Expa} + k_2 W_{Expa}^2 \tag{21}$$

where k_0, k_1, and k_2 are the coefficients.

The payback time refers to the minimum time required to compensate for the original investment cost, which is calculated as follows [31]:

$$\sum_{t=0}^{N_{ts}} (CI_t - CO_t) = 0 \tag{22}$$

where N_{ts} is the payback time.

4. Results and Discussion

In this section, the energy flexibility of the electricity load and the economic performance of the CCES system for load shifting are analyzed.

4.1. Electricity Load Energy Flexibility Analysis

Utilizing the optimization result, Figure 7 displays the initial electricity load and the electricity load after load shifting in summer, winter, and the transition season.

It can be observed that the CCES system charges during periods of low electricity loads and discharges during periods of high electricity loads. Therefore, the electricity load in peak periods is shifted to off-peak periods, resulting in a smoother electricity load. After load shifting, the standard deviation of the electricity load decreases from 76.3, 66.2, and 71.6 to 33.9, 46.1, and 34.0, which are decreased by 55.6%, 30.4%, and 52.5%, in summer, winter, and the transition season, respectively. However, due to the restriction of the SOC of the CCES system, the CCES system is unable to maintain charging at a constant electric capacity during periods of low electricity loads. It is also unable to continue discharging a stable electric capacity during high electricity loads. This causes the new volatility of the electricity load at periods of low and high electricity loads, respectively, compared to the initial electricity load. Simultaneously, it was observed that the deployment of the CCES system for load shifting induces abrupt changes in the electricity load. This issue could be effectively addressed by integrating a new energy storage system characterized by higher power density, such as battery and supercapacitor energy storage systems.

Table 2 summaries the energy flexibility of the electricity load after load shifting by the CCES system.

Table 2. The energy flexibility of the electricity load in three seasons.

Flexibility Indicators	Summer	Winter	Transition Season
$W_{fmax,up}$ (MW)	93	90	99
$E_{f,up}$ (MWh)	3845	4052	3816
$W_{fmax,down}$ (MW)	120	108	120
$E_{f,down}$ (MWh)	3846	3180	3735

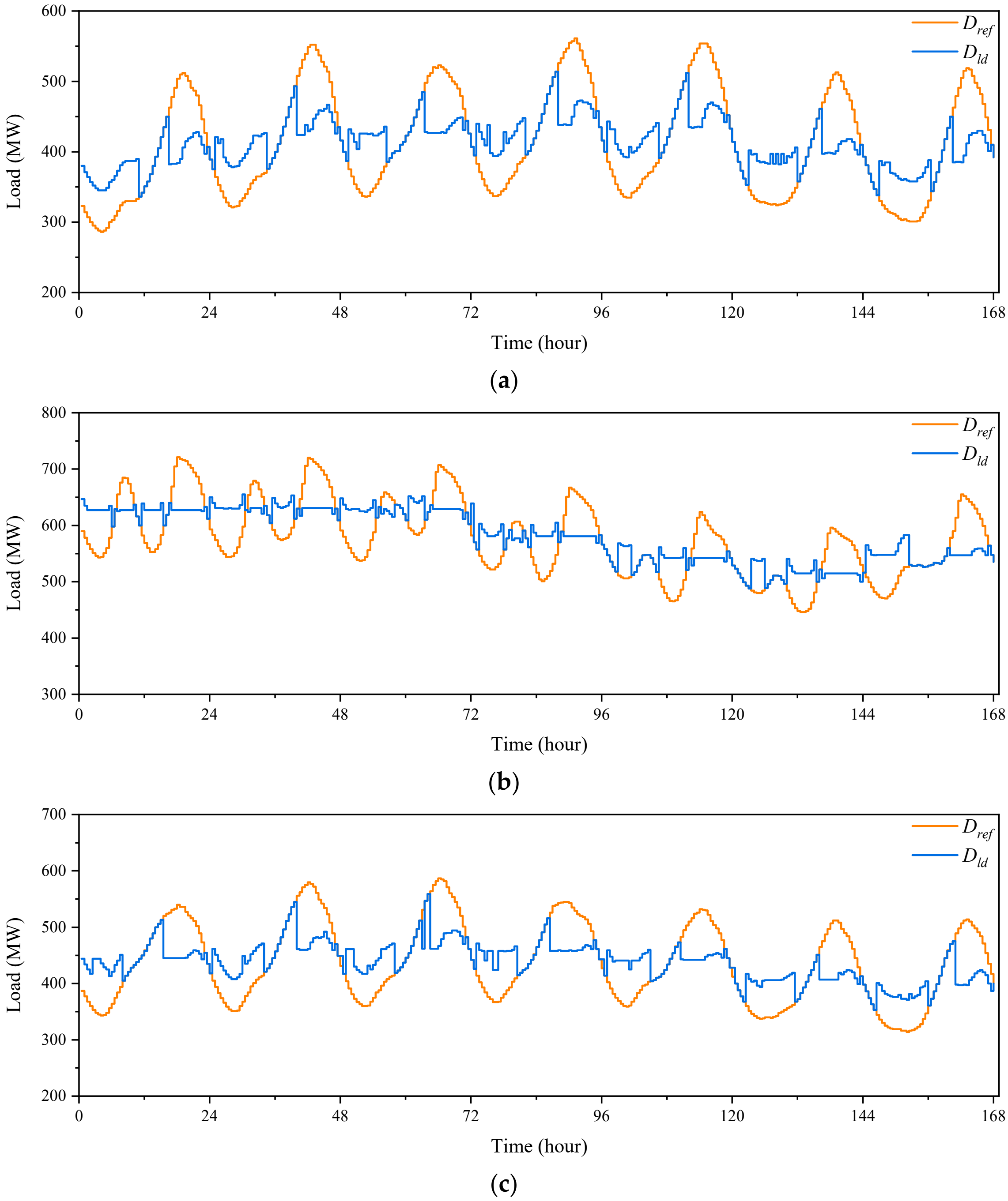

Figure 7. The initial electricity load and the electricity load after load shifting by the CCES system. (**a**) The initial electricity load and the electricity load after load shifting in summer. (**b**) The initial electricity load and the electricity load after load shifting in winter. (**c**) The initial electricity load and the electricity load after load shifting in the transition season.

As indicated in Table 2, the maximum upward flexible capacity of the electricity load after load shifting stands at 99 MW, which is below the compressor's maximum electric capacity of 110 MW. This arises from the longer charging duration and the higher SOC associated with the compressor's lower electric capacity, allowing the CCES system to discharge at a higher electric capacity. Consequently, the CCES system does not operate at the maximum electric capacity to ensure a smoother electricity load. It is noteworthy that the maximum downward flexible capacity of the electricity load matches the maximum electric capacity of the expander, i.e., 120 MW. Furthermore, upon successful load shifting, a maximum upward flexible energy of 3845 MWh and a maximum downward flexible energy of 3846 MWh are provided by the electricity load.

The energy storage capacity of the CCES system has a significant influence on the energy flexibility of the electricity load. The sensitivity analysis is conducted to examine the influence of the energy storage capacity of the CCES system on the energy flexibility of the electricity load. Figure 8 shows the upward and downward flexibility of the electricity load when the energy storage capacity of the CCES system varies in the range from −20% to 20%.

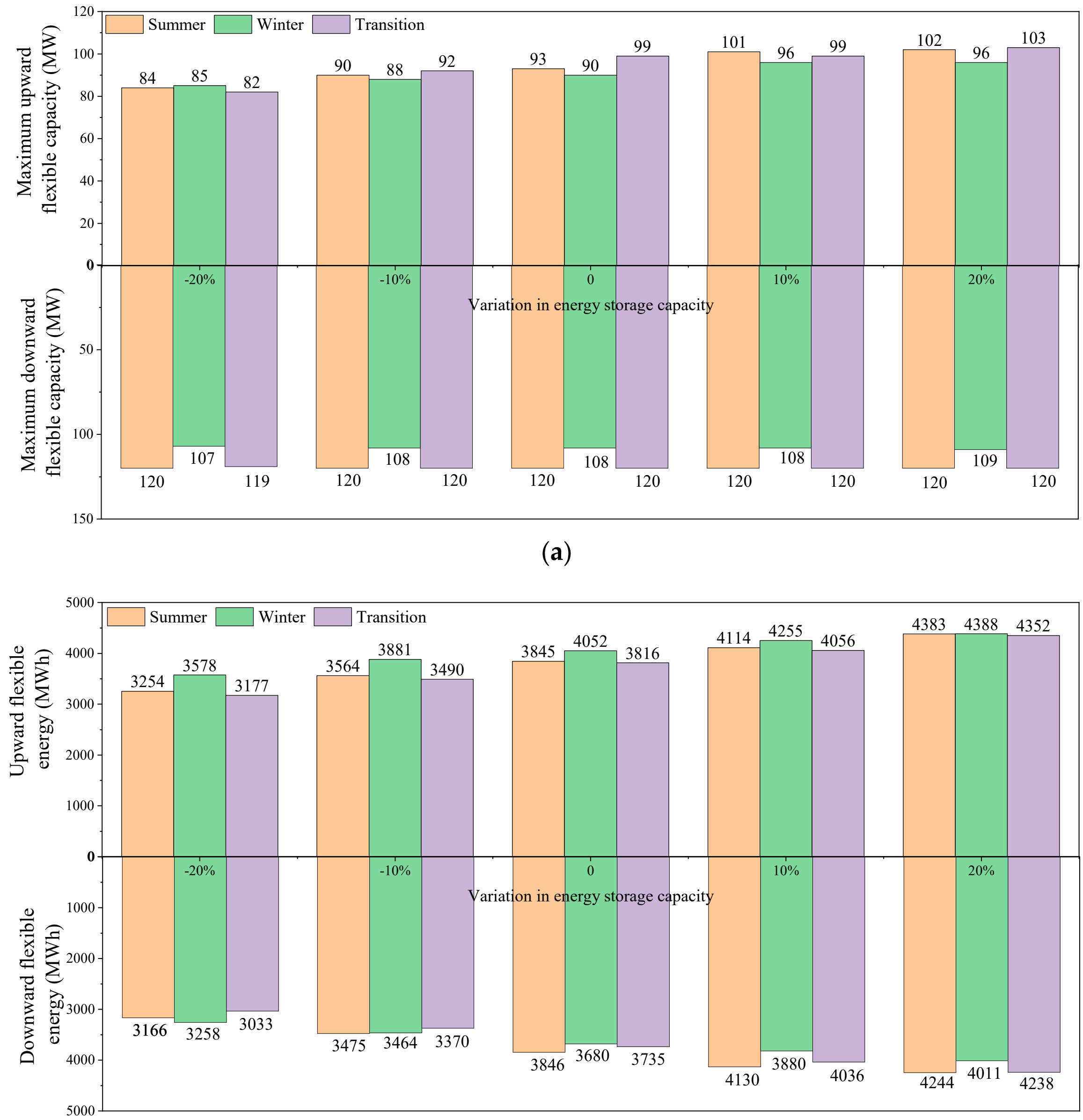

(**a**)

(**b**)

Figure 8. Effects of the energy storage capacity of the CCES system on the energy flexibility of the electricity load. (**a**) Effects of the energy storage capacity of the CCES system on the maximum upward and downward flexible capacities of the electricity load. (**b**) Effects of the energy storage capacity of the CCES system on the upward and downward flexible energies of the electricity load.

As depicted in Figure 8a, there is an increase in the maximum upward flexible capacity as the energy storage capacity increases. This phenomenon is attributed to the elongation of the discharging time, necessitating a greater amount of compressed CO_2 when the energy storage capacity increases. Consequently, the CCES system operates at a higher electricity capacity to ensure the desired amount of CO_2 is achieved. With an increase in the energy storage capacity of the CCES system, the maximum electric capacity of the expander remains constant, resulting in a consistent maximum downward flexibility capacity. Additionally, the rises in both charging capacity and discharging time lead to an elevation in both upward and downward flexible energies as the energy storage capacity of the CCES system increases.

4.2. Economic Performance Analysis

When employing the energy storage system for load shifting purposes, the CCES system can generate income through energy arbitrage and coal reduction. The incomes of the CCES system during a week in summer, winter, and the transition season are summarized in Table 3.

Table 3. The incomes of the CCES system during a week in three seasons.

Season	Income (MUSD)
Summer	0.63
Winter	0.29
Transition	0.37

It can be observed that the CCES system generates the lowest income of MUSD 0.29 in the winter. This is due to the smoother electricity price and load in winter, as shown in Figure 2. Based on the income of the CCES system in each season, the annual income of the CCES system can be determined, which is MUSD 21.2. Assuming an annual income equivalent to that of 2022 and a discount rate of 7%, the NPV of the CCES system is shown in Figure 9.

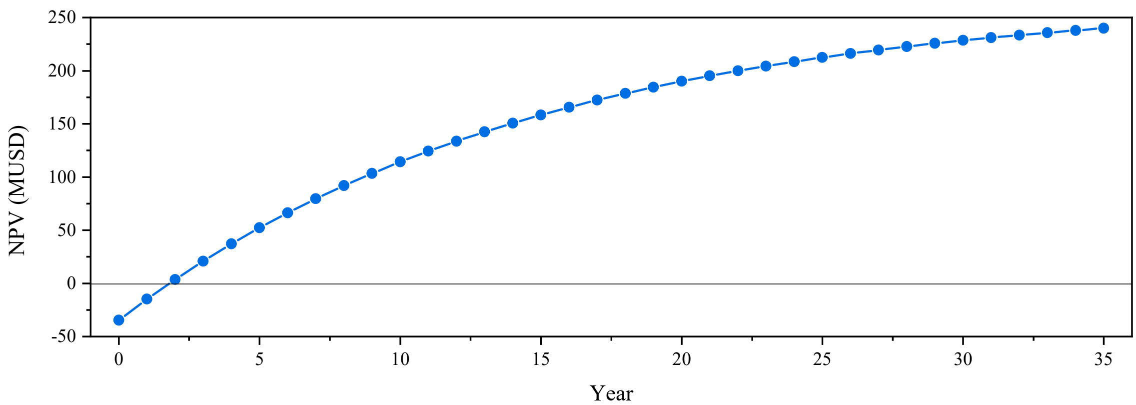

Figure 9. The NPV of the CCES system at a discount rate of 7%.

According to Figure 9, the NPV of the CCES system becomes positive from the second year, which implies the payback time of the CCES system is less than 3 years. The NPV accumulates a total of MUSD 239.9 over the entire project lifespan, which is 35 years. Based on the findings, it can be concluded that the utilization of the CCES system to achieve load shifting is economically viable.

The energy storage capacity of the CCES system has a significant influence on the income of the CCES system. The sensitivity analysis is conducted to examine the influence of the energy storage capacity of the CCES system on the income of the CCES system. Figure 10 shows the income and the NPV of the CCES system when the energy storage capacity of the CCES system varies in the range from −20% to 20%.

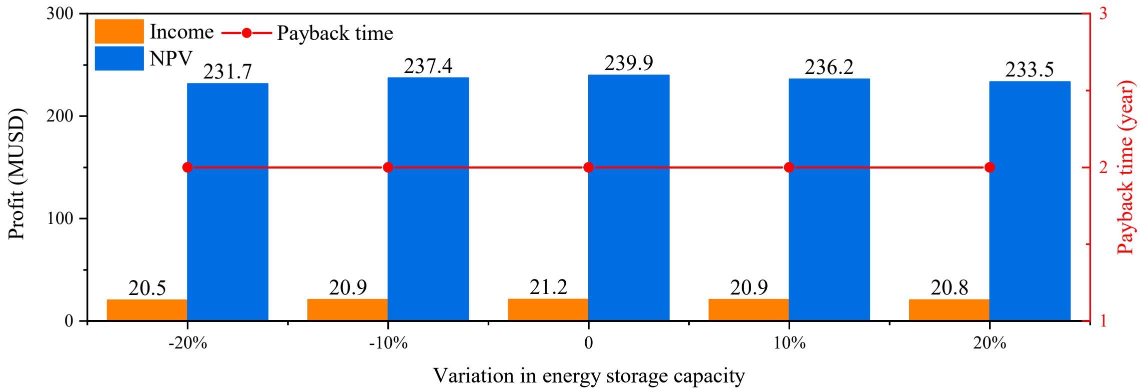

Figure 10. Effects of the energy storage capacity of the CCES system on the income and the NPV of the CCES system.

From Figure 10, an observable trend emerges wherein the income and the NPV of the CCES system initially rise and subsequently decline as the energy storage capacity of the CCES system increases. When maintaining an unchanged energy storage capacity of 267 MWh, the CCES system achieves its peak income and NPV values, reaching MUSD 21.2 and MUSD 239.9, respectively. When the energy storage capacity varies within the range of −20% to 0%, the extended discharging time results in an increase of 1.8 GW in the electricity energy from the expander, surpassing the increase of 1.7 GW from the compressor's electricity energy. Meanwhile, the investment cost of the CCES system only increases MUSD 1.0. Consequently, the income and the NPV of the CCES system follow upward trajectories with increasing energy storage capacity. Nevertheless, when the energy storage capacity varies from 0% to 20%, in pursuit of maintaining a smoother electricity load, the growth in discharging time becomes slow. Consequently, the augmented electricity energy of the expander is 1.2 GW, falling below the 1.4 GW increase from the compressor's electricity energy. This leads to an elevation in electricity purchasing expenses and a subsequent decline in the CCES system's income as the energy storage capacity of the CCES system increases.

As discussed earlier, the CCES system demonstrates favorable techno-economic performance for load shifting. Nonetheless, the direct utilization of the CCES system for load shifting introduces certain drawbacks, such as new volatility and abrupt fluctuations in the electricity load. To address this challenge, a hybrid energy storage system that specifically integrates the CCES system with a battery energy storage system can be employed. In this hybrid configuration, the CCES system manages lower frequency, higher amplitude variations in electricity load, while the battery energy storage system handles higher frequency, lower amplitude variations. Future research should focus on developing control strategies and electricity capacity dispatch mechanisms for the hybrid energy storage system.

5. Conclusions

This paper proposes the use of the compressed CO_2 energy storage (CCES) system to achieve load shifting, which provides energy flexibility of the electricity load and creates energy arbitrage from variations in the electricity prices. By optimizing the operation of the CCES system for load shifting and conducting an associated sensitivity analysis, the following conclusions have been drawn.

With an energy storage capacity of 267 MWh, the CCES system during a week in summer, winter, and the transition season provides 3845 MWh, 4052 MWh, and 3816 MWh of upward flexible energy and 3846 MWh, 3180 MWh, and 3735 MWh of downward flexible energy, respectively. The sensitivity analysis indicates that a 20% increase in energy storage capacity results in 14.0%, 8.3%, and 14.0% increases in upward flexible energy and 10.3%, 9.0%, and 13.5% increases in downward flexible energy in summer, winter, and the transition season, respectively.

With an energy storage capacity of 267 MWh, the CCES system can attain a net present value (NPV) of MUSD 239.9 over a lifespan of 35 years and a payback time of 2 years. The sensitivity analysis shows that, when maintaining an unchanged energy storage capacity, the CCES system achieves its peak income and NPV.

Author Contributions: Methodology, J.Y.; Software, W.W.; Investigation, X.R.; Resources, S.T. and Q.S.; Writing—original draft, B.Z.; Writing—review & editing, Q.H. All authors have read and agreed to the published version of the manuscript.

Funding: This work was financed by the Shandong Electric Power Engineering Consulting Institute Foundation of China (Grant No. 37-K2021-124).

Data Availability Statement: Data are contained within the article.

Conflicts of Interest: Author Bin Zhang, Junbo Yang and Sule Tian were employed by the company Shandong Electric Power Engineering Consulting Institute Co., Ltd. The remaining authors declare that the research was conducted in the absence of any commercial or financial relationships that could be construed as a potential conflict of interest.

References

1. Kebede, A.A.; Kalogiannis, T.; Van Mierlo, J.; Berecibar, M. A comprehensive review of stationary energy storage devices for large scale renewable energy sources grid integration. *Renew. Sustain. Energy Rev.* **2022**, *159*, 112213. [CrossRef]
2. Budt, M.; Wolf, D.; Span, R.; Yan, J. A review on compressed air energy storage: Basic principles, past milestones and recent developments. *Appl. Energy* **2016**, *170*, 250–268. [CrossRef]
3. Luo, X.; Wang, J.; Dooner, M.; Clarke, J. Overview of current development in electrical energy storage technologies and the application potential in power system operation. *Appl. Energy* **2015**, *137*, 511–536. [CrossRef]
4. Wang, W.; Sun, B.; Li, H.; Sun, Q.; Wennersten, R. An improved min-max power dispatching method for integration of variable renewable energy. *Appl. Energy* **2020**, *276*, 115430. [CrossRef]
5. Krishan, O.; Suhag, S. An updated review of energy storage systems: Classification and applications in distributed generation power systems incorporating renewable energy resources. *Int. J. Energy Res.* **2019**, *43*, 6171–6210. [CrossRef]
6. Guo, C.; Xu, Y.; Guo, H.; Zhang, X.; Lin, X.; Wang, L.; Zhang, Y.; Chen, H. Comprehensive exergy analysis of the dynamic process of compressed air energy storage system with low-temperature thermal energy storage. *Appl. Therm. Eng.* **2019**, *147*, 684–693. [CrossRef]
7. Tong, Z.; Cheng, Z.; Tong, S. A review on the development of compressed air energy storage in China: Technical and economic challenges to commercialization. *Renew. Sustain. Energy Rev.* **2021**, *135*, 110178. [CrossRef]
8. Zhang, Y.; Yao, E.; Tian, Z.; Gao, W.; Yang, K. Exergy destruction analysis of a low-temperature Compressed Carbon dioxide Energy Storage system based on conventional and advanced exergy methods. *Appl. Therm. Eng.* **2021**, *185*, 116421. [CrossRef]
9. Liu, H.; Wei, Z.; He, W.; Zhao, J. Thermal issues about Li-ion batteries and recent progress in battery thermal management systems: A review. *Energy Convers. Manag.* **2017**, *150*, 304–330. [CrossRef]
10. Huang, Q.; Yao, J.; Hu, Y.; Liu, S.; Li, H.; Sun, Q. Integrating compressed CO_2 energy storage in an oxy-coal combustion power plant with CO_2 capture. *Energy* **2022**, *254*, 124493. [CrossRef]
11. Liu, S.; Wu, S.; Hu, Y.; Li, H. Comparative analysis of air and CO_2 as working fluids for compressed and liquefied gas energy storage technologies. *Energy Convers. Manag.* **2019**, *181*, 608–620. [CrossRef]
12. Jia, L.; Chen, H.; Xu, Y.; Liang, W.; Tan, C. A solar energy storage and power generation system based on supercritical carbon dioxide. *Renew. Energy* **2014**, *64*, 43–51.
13. Liu, H.; He, Q.; Borgia, A.; Pan, L.; Oldenburg, C.M. Thermodynamic analysis of a compressed carbon dioxide energy storage system using two saline aquifers at different depths as storage reservoirs. *Energy Convers. Manag.* **2016**, *127*, 149–159. [CrossRef]
14. Hao, Y.; He, Q.; Du, D. A trans-critical carbon dioxide energy storage system with heat pump to recover stored heat of compression. *Renew. Energy* **2020**, *152*, 1099–1108. [CrossRef]
15. Xu, M.; Zhao, P.; Huo, Y.; Han, J.; Wang, J.; Dai, Y. Thermodynamic analysis of a novel liquid carbon dioxide energy storage system and comparison to a liquid air energy storage system. *J. Clean. Prod.* **2020**, *242*, 118437. [CrossRef]
16. Wang, M.; Zhao, P.; Wu, Y.; Dai, Y. Performance analysis of a novel energy storage system based on liquid carbon dioxide. *Appl. Therm. Eng.* **2015**, *91*, 812–823. [CrossRef]
17. Huang, Q.; Feng, B.; Liu, S.; Ma, C.; Li, H.; Sun, Q. Dynamic operating characteristics of a compressed CO_2 energy storage system. *Appl. Energy* **2023**, *341*, 120985. [CrossRef]
18. Zhang, Y.; Wu, Y.; Yang, K. Dynamic characteristics of a two-stage compression and two-stage expansion Compressed Carbon dioxide energy storage system under sliding pressure operation. *Energy Convers. Manag.* **2022**, *254*, 115218. [CrossRef]
19. Chaychizadeh, F.; Dehghandorost, H.; Aliabadi, A.; Taklifi, A. Stochastic dynamic simulation of a novel hybrid thermal-compressed carbon dioxide energy storage system (T-CCES) integrated with a wind farm. *Energy Convers. Manag.* **2018**, *166*, 500–511. [CrossRef]

20. Vazquez, S.; Lukic, S.M.; Galvan, E.; Franquelo, L.G.; Carrasco, J.M. Energy storage systems for transport and grid applications. *IEEE Trans. Ind. Electron.* **2010**, *57*, 3881–3895. [CrossRef]
21. Han, X.; Ji, T.; Zhao, Z.; Zhang, H. Economic evaluation of batteries planning in energy storage power stations for load shifting. *Renew. Energy* **2015**, *78*, 643–647. [CrossRef]
22. Parra, D.; Norman, S.A.; Walker, G.S.; Gillott, M. Optimum community energy storage system for demand load shifting. *Appl. Energy* **2016**, *174*, 130–143. [CrossRef]
23. Yan, Z.; Zhang, Y.; Liang, R.; Jin, W. An allocative method of hybrid electrical and thermal energy storage capacity for load shifting based on seasonal difference in district energy planning. *Energy* **2020**, *207*, 118139. [CrossRef]
24. Ding, Y.; Lyu, Y.; Lu, S.; Wang, R. Load shifting potential assessment of building thermal storage performance for building design. *Energy* **2022**, *243*, 123036. [CrossRef]
25. Sciacovelli, A.; Vecchi, A.; Ding, Y. Liquid air energy storage (LAES) with packed bed cold thermal storage–From component to system level performance through dynamic modelling. *Appl. Energy* **2017**, *190*, 84–98. [CrossRef]
26. Huang, Q.; Wang, W.; Ma, C.; Feng, B.; Sun, Q.; Li, H.; Wennersten, R. Assessment of the arbitrage by a compressed CO_2 energy storage system—Based on dynamic modelling. *Adv. Appl. Energy* **2023**. [CrossRef]
27. Bao, G.; Lu, C.; Yuan, Z.; Lu, Z. Battery energy storage system load shifting control based on real time load forecast and dynamic programming. In Proceedings of the 2012 IEEE International Conference on Automation Science and Engineering (CASE), Seoul, Republic of Korea, 20–24 August 2012.
28. CAISO. California ISO Today's Outlook. Available online: https://www.caiso.com/TodaysOutlook/Pages/default.aspx (accessed on 25 July 2023).
29. Zhang, K.; Kummert, M. Evaluating the impact of thermostat control strategies on the energy flexibility of residential buildings for space heating. In *Building Simulation*; Springer: Berlin/Heidelberg, Germany, 2021.
30. Zhang, H.; Zhao, J. Joint peak shaving energy consumption optimization model and simulation analysis of pumped storage power unit and coal-fired power units. *Chem. Eng. Trans.* **2016**, *51*, 1279–1284.
31. Zhou, Q.; He, Q.; Lu, C.; Du, D. Techno-economic analysis of advanced adiabatic compressed air energy storage system based on life cycle cost. *J. Clean. Prod.* **2020**, *265*, 121768. [CrossRef]